ISSN: 2449 - 0539
BAYERO JOURNAL OF ENGINEERING AND TECHNOLOGY VOL 18 NO. 2 MAY 202 PP. 104-112

# MATHEMATICAL MODELLING OF SINGLE SLOPE SOLAR STILL WITH AMBIENT TEMPERATURE AND GLOBAL IRRADIANCE

**Mohammed Tajudeen Jimoh**[1]

[1]Department of Mechanical Engineering, Bayero University, Kano, Nigeria.

## ABSTRACT

*This work models a single slope solar still. The ordinary differential equation describing the operations of the still are presented. In addition, the models for the two major inputs of the still, the ambient temperature and the global irradiance, are presented. The mathematical models provide for the study of the effects of many variables on the performance indicators of the solar still - the distillate yield, the water temperature. The variables include depth of water in the still basin, seasons of the year, slope of glass cover, and many variables of construction such as type of glass cover, insulation type and thickness.*

Keywords: Solar still; Solar still model; global irradiance model; heat transfer coefficients; ambient temperature model

# 1. INTRODUCTION

Most regions of the world, especially in Africa, have no good sources of fresh water. The only available water sources are either germs infested or are too salty, making them unfit for drinking. In these situations, water distillation can be of significant assistance. Distillation is a process whereby water is allowed to evaporate at elevated fluid temperature, and the water vapour condensed and collected in another unit. The distillate is very pure, devoid of germs and salt. Distillation requires energy source, which can be from conventional sources such as fossil fuel (either directly or as electricity) or from alternative sources such as fuel wood, solar energy etc.

Electricity is scarce and expensive and not available in many rural areas. Fossil fuel is expensive and its supply limited and for most part exhaustible. Oil is precious and in the words of Sheik Yamani (McMullan, *et al*., 1990), 'Oil is too precious to burn'. Direct use of fuel wood or fossil fuel can cause environmental pollution in the form of thermal pollution, air pollution, water pollution and climatic changes. Solar distillation, despite being low grade, is devoid of all the shortcomings mentioned above. The use of solar energy for distillation is well suited for the rural regions, requiring simple technology and maintenance.

A typical single slope solar still consists of a blackened basin containing water at a shallow depth, over which is a transparent vapour tight cover that completely encloses the space above the basin. The cover is sloped towards the collection channel. The space between the inner surface of the basin and the outside is lagged to reduce heat losses. In operation, the water receives solar radiation through the transparent cover by absorption and transmission. The transparent cover is essentially opaque to the long wave irradiance from the basin interior. It is this 'greenhouse effect' that enables temperatures significantly above ambient to be achieved inside the basin. Increase in water temperature fastens evaporation rate. The water vapour is carried upwards by thermal convection, where it condenses on the cool cover. The condensed water drops, then slides down the cover into the catchment trough.

Research approaches in solar still can be wholly empirical, or modelling and simulation, or a combination of the two. The modelling and simulation approach has gained widespread attention, due mainly to the advances in computing. Since the pioneering works of (Dunkle, 1961), (Lof, *et al*., 1961), (Frick, 1970), (Nayak, *et al*., 1980) and others in the area of solar distillation modelling, and that of (Cooper, 1969) in digital simulation, many other works in these fields have followed. Among the follow-up works are those of (Dwivedi & Tiwari, 2009), (El-Sebaila & Al-Dossarib, 2011), (Gupta, *et al*., 2013), (Yeo, *et al*., 2014), (Torchia-Núñez, et al., 2014). Other also devoted solely to modelling and simulation are (Ebaid & Ammari, 2015) and (Johnson, *et al*., 2019).

Some of these works make many assumptions which are largely responsible for the wide gap between empirical results and simulation predictions. Some works treat the solar distillation process as a steady state analysis rather than transient-state analysis. Others proposed that the solar distillation process may be described using only one Ordinary Differential Equation (ODE). Recent literatures and better understanding of heat transfer process show that a minimum of three ODE is required to describe the solar distillation process. See for example (Duffie & Becham, 2013).

ISSN: 2449 - 0539
BAYERO JOURNAL OF ENGINEERING AND TECHNOLOGY VOL 18 NO. 2 MAY 202 PP. 104-112

This work carries out a simulation study of single basin solar still. It presents the mathematical model governing the energy balance in the still. It also presents the mathematical models for estimating the ambient temperature and the global radiance, the major input variables of the still. The models allow for the study of the effects of parameters and variables such as ambient temperature, solar irradiance, water depth, on the still performance. This study adopts a transient state analysis rather than a simpler but less encompassing steady-state analysis adopted in some previous works. It accounts for change in water mass in the still with time. The specific heat capacities of the glass cover and basin are accounted for, while the difference in areas of cover glass and still and water surface are also considered.

# 2. MATERIALS AND METHODS

### 2.1 Models of single slope solar still

The heat and mass transfer process in a solar still is governed by its interaction with the solar irradiance and its environment (ambient temperature and air). Figure 1 illustrates the relationships between the solar irradiance incident on a single basin solar still, and of energy transfer within it.

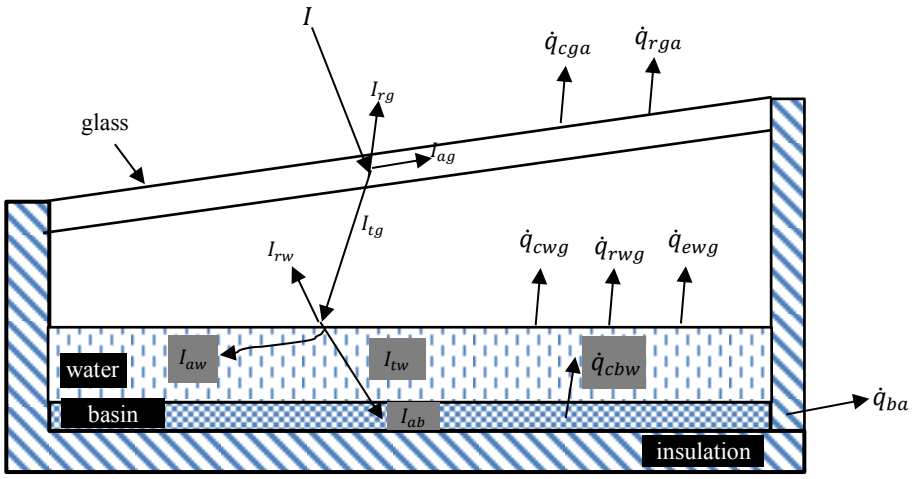


Figure 1: Energy transfer components in a typical single slope solar still (not all features of the solar still shown)

As shown in the figure, part of the global irradiance reaching the still glass cover ($I$) is reflected ($I_{rg}$) or absorbed ($I_{ag}$) by it, while the remainder is transmitted ($I_{tg}$ ) through it. Of the transmitted irradiance through the cover, part of it is reflected from the water surface ($I_{rw}$), and a part of it is absorbed ($I_{aw}$) in the water itself. The remaining is transmitted through the water ($I_{tw}$) to the bottom absorber. Most of the radiation incident on the basin bottom ($I_{ab}$) is absorbed by convection by the water ($\dot{q}_{cbw}$), thereby raising its temperature. As a result of temperature difference between the water and the cover, energy is transferred from water to cover by convection ($\dot{q}_{cwg}$), radiation ($\dot{q}_{rwg}$) and evaporation ($\dot{q}_{ewg}$). The solar still also loses energy by convection ($\dot{q}_{cga}$) and radiation ($\dot{q}_{rga}$) to the ambient air, and by combined conduction and convection ($\dot{q}_{ba}$) through the bottom, to the ambient.

The heat and mass transfer models of the solar still are obtained using the energy balance approach. The key assumptions in the modelling of the energy balance of solar still are that (i) there is no vapour leakage in the still; (ii) that the temperature gradient in glass thickness, water depth and basin thickness are neglected; (iii) that the variation of latent heat of vaporisation of water with temperature are neglected; and (iv) that the heat capacity of the insulation is neglected.

Bearing in mind the above assumptions, the energy balance in a solar still can be divided into three categories: energy balance for glass cover, energy balance for water mass in basin, and energy balance for basin Liner. The energy balances are defined as follows:

#### *2.1.1 Energy Balance for Glass Cover*

With reference to Figure 1 and applying the energy conservation principle, the energy balance for glass cover can be written as (Torchia-Núñez, et al., 2014):

$$m_g C_{pg} \frac{dT_g}{dt} = \underbrace{\left[A_g I_{ag} + A_w\left(\dot{q}_{cwg} + \dot{q}_{ewg} + \dot{q}_{rwg}\right)\right]}_{heat\ gain} - \underbrace{A_g\left(\dot{q}_{cga} + \dot{q}_{rga}\right)}_{heat\ loss} \quad (1)$$

Equation (1) says that the rate of change of the energy of the glass cover is equal to the heat gained by the glass

(from water and solar irradiance) minus heat loss by the glass (to the environment). In the equation, $T_g$, $m_g$, and $C_{pg}$ are the glass temperature, mass, and specific heat capacity respectively. It can be shown that the surface are of the glass ($A_g$), surface area of water ($A_w$), and mass of the glass ($m_g$) can be approximated as:

$$A_g = L_s B_s sec\theta \quad (2)$$

$$A_w = L_s B_s \quad (3)$$

$$m_g = A_g \rho_g t_g \quad (4)$$

where $\rho_g$, $t_g$, and $\theta$ are the glass density, thickness, and tilt angle respectively, while $L_s$ and $B_s$ are the length and breadth of the still.

**Heat gain by glass cover**

With respect to figure 1 and equation 1, the total heat gain by the glass cover is the sum of convective, radiative and, evaporative heat transfer from water, as well as absorbed solar irradiance. The convective heat flux from water to glass is $\dot{q}_{cwg} = h_{cwg}(T_w - T_g)$, where $h_{cwg}$ is convective heat transfer coefficient between the water surface and the glass is given as (Tiwari, 2002):

$$h_{cwg} = (Gr_v Pr_v)^{n_v}(k_v C_v)/d_{wg} \quad (5)$$

where $d_{wg}$ is the average spacing between water surface and glass cover, and $Gr_v$ and $Pr_v$ in equation (5) are defined as in Table 1.

Table 1: Expressions for calculating $\boldsymbol{Gr_v}$ and $\boldsymbol{Pr_v}$ for moist air (Tiwari, 2002)

| Dimensionless numbers | Symbol | Expressions |
|---|---|---|
| Grashof number for moist air | $Gr_v$ | $\left[(g\beta_v d_{wg}^3 \rho_v^2)/\mu_v^2\right]\Delta TP$ |
| Prandtl number for moist air | $Pr_v$ | $\mu_v C_{pv}/k_v$ |

The values of the constants $C_v$ and $n_v$ in equation (5) depend on $d_{wg}$, as shown in Table 2.

Table 2: Values of $\boldsymbol{C_v}$ and $\boldsymbol{n_v}$ for different water- glass cover spacing (Dunkle, 1961) (Tiwari, 2002)

| $d_{wg}$ | $C_v$ | $n_v$ |
|---|---|---|
| 0.15 | 0.21 | 0.25 |
| 0.20 | 0.21 | 0.25 |
| 0.25 | 0.075 | 1/3 |

The moist air properties ($\mu_v$ - dynamic viscosity; $C_{pv}$ - specific heat capacity; $k_v$ - thermal conductivity; $\beta_v$ - thermal expansivity, and $\rho_v$ - density) inside the basin can be obtained from Table 3. The moisture properties are determined at temperature $T_v = 0.5(T_w + T_g)$.

The corrected temp difference, $\Delta TP$, is given as:

$$\Delta TP = \left[T_w - T_g + (P_w - P_g)T_w/(268.9 \times 10^3 - P_w)\right] \quad (6)$$

Table 3: Expressions for calculating temperature dependent properties of moist air (Tiwari, 2002)

| Properties | Evaluation Expressions |
|---|---|
| $\mu_v$ | $1.718 \times 10^{-5} + 4.62 \times 10^{-8} T_v$ |
| $C_{pv}$ | $999.2 + 0.1434 T_v + 1.101 \times 10^{-4} T_v^2 - 6.7581 \times 10^{-8} T_v^3$ |
| $k_v$ | $0.0244. + 0.7673 \times 10^{-4} T_v$ |
| $\beta_v$ | $1/(T_v + 273.15)$ |
| $\rho_v$ | $353.44/(T_v + 273.15)$ |

The evaporative heat flux from water to glass is $\dot{q}_{ewg} = h_{ewg}(T_w - T_g)$, where $h_{ewg}$ is evaporative heat transfer coefficient between the water surface and the glass is given as (Tiwari, 2002):

$$h_{ewg} = 0.016273 h_{cwg}(P_w - P_g)/(T_w - T_g) \quad (7)$$

The partial pressures of vapour $P_x$ (i.e. $P_w$ or $P_g$) at a temperature $T_x$ (in Kelvin) is expressed as (Fernandez & Chargoy, 1990):

$$P_x = exp(25.317 - 5144/T_x) \quad (8)$$

The radiation heat flux from water to glass is $\dot{q}_{rwg} = h_{rwg}(T_w - T_g)$, where $h_{rwg}$ is radiation heat transfer coefficient between the water surface and the glass is given as (Tiwari, 2002):

$$h_{rwg} = \varepsilon_f \sigma\left[{T_w}^2 + {T_g}^2\right](T_w + T_g) \quad (9)$$

where $\varepsilon_f$ is the effective emissivity given as $\varepsilon_f = \left[(1/\varepsilon_g + 1/\varepsilon_w) - 1\right]^{-1}$, and $\varepsilon_w$ is emissivity of water.

**Heat loss by glass cover**

The total heat loss by the glass cover is the sum of convective and radiative heat transfers from glass cover to air. The convective heat flux from glass to air is $\dot{q}_{cga} = h_{cga}(T_g - T_a)$, where $h_{cga}$ is the natural convective heat transfer coefficient from glass to air defined as (Watmuff, et al., 1977) (Tiwari, 2002)

$$h_{cga} = 2.8 + 3v_a \quad (10)$$

where $v_a$ is the ambient wind velocity.

The radiative heat flux from glass to air is $\dot{q}_{rga} = h_{rga}(T_g - T_a)$, where $h_{rga}$ is the radiation heat transfer coefficient from glass to air defined as (Tiwari, 2002):

$$h_{rga} = \varepsilon_g \sigma\left({T_g}^4 - {T_{sky}}^4\right)/\left(T_g - T_{sky}\right) = \varepsilon_g \sigma\left[{T_g}^2 + {T_{sky}}^2\right]\left(T_g + T_{sky}\right) \quad (11)$$

where $\varepsilon_g$ is glass emissivity and $\sigma$ is Stephan Boltzmann constant ($\sigma = 5.67 \times 10^{-8}\ W/m^2K^4$). The sky temperature $T_{sky}$ is given as (Tiwari, 2002):

$$T_{sky} = T_a - 12 \quad (12)$$

where $T_a$ is the ambient temperature.

By defining the total heat transfer coefficient from glass to air as $h_{wg} = h_{cwg} + h_{ewg} + h_{rwg}$, and total heat transfer coefficient from water to glass as $h_{ga} = h_{cga} + h_{rga}$, the energy balance equation (1) can be re-written as:

$$\frac{dT_g}{dt} = \frac{1}{m_g C_{pg}}\left[A_g I_{ag} + A_w h_{wg}(T_w - T_g) - A_g h_{ga}(T_g - T_a)\right] \quad (13)$$

### *2.1.2 Energy Balance for Water mass in Basin*

Again, with reference to figure 1 and applying the conservation of energy principle, the energy balance equation for water mass in the basin can be written as (Tiwari, 2002), (Torchia-Núñez, et al., 2014):

$$m_w C_{pw}\frac{dT_w}{dt} = \underbrace{(A_w I_{aw} + A_b \dot{q}_{cbw})}_{heat\ gain} - \underbrace{A_w(\dot{q}_{ewg} + \dot{q}_{cwg} + \dot{q}_{rwg})}_{heat\ loss} \quad (14)$$

Equation (14) says that the rate of change of the energy of the water mass in the basin is equal to its energy gained (from basin liner and solar irradiance) minus its energy loss (to the glass). The surface area of the basin ($A_b$) is the same as that of the water ($A_w$), and mass $m_w$ of the water can be approximated as:

$$m_w = (\rho_w L_s B_s d_w) \quad (15)$$

where $\rho_w$ and $d_w$ are density and depth of water respectively. Note that $d_w$ varies with time.

**Heat gain by water**

The total heat gain by water (brine) is the sum of absorbed irradiance by water and convective heat transfers from basin to water.

The convective heat flux from basin to the water is $\dot{q}_{cbw} = h_{cbw}(T_b - T_w)$, where $h_{cbw}$ is the convective heat transfer coefficient between the basin liner and the water, and is given as (Tiwari, 2002):

$$h_{cbw} = \left(k_f C_f / x_f\right)\left(Gr_f Pr_f\right)^{n_f} \quad (16)$$

where, assuming the flow is laminar, the constants $C_f$ and $n_f$ are 0.54 and 0.25 respectively (Tiwari, 2002):

The $Gr_f$, $Pr_f$ and $x_f$ (Grashof number, Prandtl number and characteristic lengths respectively) are defined for the pair of surfaces as in Table 4.

For the equations in Table 4, the properties of water ($\mu_f$ - dynamic viscosity; $C_{pf}$ - specific heat capacity; $k_f$ - thermal conductivity; $\beta_f$ - thermal expansivity, and $\rho_f$ - density) are determined at temperature $T_f = 0.5(T_b + T_w)$ and can be obtained using the expressions in Table 5.

**Heat loss by water**

The total heat loss by water sum of convective, radiative and, evaporative heat transfer from it, and they are as presented earlier.

Table 4: Equations for calculating $Gr_f$, $Pr_f$ and $x_f$ for water (saturated liquid) (Tiwari, 2002)

| Terms | Expressions |
|---|---|
| $Gr_f$ | $\left(\frac{g\beta_f x_f^3 \rho_f^2}{\mu_f^2}\right)(T_b - T_w)$ |
| $Pr_f$ | $\frac{\mu_f C_{pf}}{k_f}$ |
| $x_f$ | $\begin{cases} (L+B)/2, & 10^5 < Gr_f Pr_f < 2\times 10^7 \\ (0.5LB)/(L+B), & 10^7 < Gr_f Pr_f < 10^{11} \end{cases}$ |

Table 5: Expressions for calculating temperature dependent properties of water (saturated liquid)

| Symbols | Evaluation Expressions |
|---|---|
| $\mu_f$ | $0.0017 - 4.6535\times 10^{-5} T_f + 5.7066 \times 10^{-7} T_f^2 - 2.5438 \times 10^{-9} T_f^3$ |
| $C_{pf}$ | $4217 - 2.9971 T_f + 0.0775 T_f^2 - 8.028 \times 10^{-4} T_f^3 + 3.2887 \times 10^{-6} T_f^4$ |
| $k_f$ | $0.56 + 0.021 T_f - 9.483 \times 10^{-6} T_f^2$ |
| $\rho_f$ | $1006 - 0.071 T_f - 0.0036 T_f^2$ |
| $\beta_f$ | $1/(T_f + 273.15)$ |

In terms of the heat transfer coefficients, the energy balance Equation (14) can be re-written as:

$$\frac{dT_w}{dt} = \frac{1}{m_g C_{pb}}\left[A_w I_{aw} + A_b h_{bw}(T_b - T_w) - A_w h_{wg}(T_w - T_g)\right] \quad (17)$$

### *2.1.3 Energy Balance for Basin Liner*

The energy balance for the basin liner therefore takes the form:

$$m_b C_{pb}\frac{dT_b}{dt} = A_b I_{ab} - (A_w \dot{q}_{cwb} + A_b \dot{q}_{ba}) \quad (18)$$

This means that the rate of change of the energy of the basin liner is equal to its energy gained (solar irradiance) minus its energy loss to the surroundings (due to conduction, convection and radiation). It can be shown that the mass $m_b$ of the basin can be expressed as:

It can be shown that the mass $m_b$ of the basin can be approximated as:

$$m_b = (\rho_b L_s B_s t_b) \quad (19)$$

where $\rho_b$ and $t_b$ are the density and thickness of the basin material respectively, and $L_s$ and $B_s$ are length and breadth of the still respectively.

The overall heat transfer coefficient (due to conduction, convection and radiation) between the basin liner and air is (Tiwari, 2002):

$$h_{ba} = [d_i/k_i + 1/(h_{cba} + h_{rba})]^{-1} \quad (20)$$

For simplicity, a combined heat transfer coefficient $h_i$ (that includes the effect of both convection and radiation heat transfer between the basin liner and air) is normally used. In this case the overall heat transfer coefficient is approximately given as:

$$h_{ba} = [d_i/k_i + 1/h_i]^{-1} \quad (21)$$

Typical values of $h_i$ range from 1 to 10 $W/m\ ^0C$

In terms of the heat transfer coefficients, the energy balance Equation (18) can be written as:

$$\frac{dT_b}{dt} = \frac{1}{m_b C_{pb}}[A_b I_{ab} - A_b h_{cwb}(T_b - T_w) - A_b h_{ba}(T_b - T_a)] \quad (22)$$

**2.2. Models of global irradiance radiation**

There are many empirical models for estimating solar irradiance. The ASHRAE clear-sky solar radiation models offer the simplest models for estimating the beam normal ($I_B$), and the diffuse ($I_D$) terrestrial irradiance, and are given respectively as (ASHRAE, 2017):

$$I_B = I_{NE} \exp(-\tau_b m_a^{ab}) \quad (23)$$

$$I_D = I_{NE} \exp(-\tau_d m_a^{ad}) \quad (24)$$

where

| | | |
|---|---|---|
| $I_{NE}$ | - | extra-terrestrial normal irradiance, $W/m^2$ |
| $m$ | - | Air mass |
| $\tau_b$ and $\tau_d$ | - | Beam and diffuse optical depths |
| $ab$ and $ab$ | - | Beam and diffuse air mass exponents |

The extra-terrestrial normal solar irradiance ($I_{NE}$) varies throughout the year, and is approximated as (Myers, 2013):

$$I_{NE} = I_{SC}\left[1 + 0.033\cos\left(\frac{360^o n}{365}\right)\right] \quad (25)$$

where $I_{SC}$ is the solar constant (with latest adopted value of 1366 W/m$^2$ (Myers, 2013)

The air mass (corrected for refracted in the atmosphere and variation in altitude) is given as (Kasten & Young, 1989):

$$m_a = [1/cos\theta_Z + 0.50572(96.07995 - \theta_Z)^{-1.6364}] \quad (26)$$

The Beam and diffuse optical depths are location specific and vary during the year. The values tabulated for the 21$^{st}$ day of each month are as given in table 6:

The Beam and diffuse air mass exponents are obtained through the following empirical relationships (ASHRAE, 2017):

$$ab = 1.454 - 0.406\tau_b - 0.268\tau_d + 0.021\tau_b\tau_d \quad (27)$$

$$ad = 0.507 + 0.205\tau_b - 0.080\tau_d - 0.190\tau_b\tau_d \quad (28)$$

The Zenith angle ($\theta_Z$) can be calculated from the expression (Myers, 2013):

$$cos\theta_Z = sin\delta sin\phi + cos\delta cos\omega cos\phi \quad (29)$$

Table 6: Values of beam and diffuse optical depths for the 21$^{st}$ day of months in the year **(ASHRAE, 2017)**

| Month Name | Month No | $\tau_b$ | $\tau_d$ |
|---|---|---|---|
| Jan | 1 | 0.310 | 2.538 |
| Feb | 2 | 0.315 | 2.521 |
| Mar | 3 | 0.347 | 2.453 |
| Apr | 4 | 0.386 | 2.324 |
| May | 5 | 0.440 | 2.213 |
| Jun | 6 | 0.473 | 2.168 |
| Jul | 7 | 0.515 | 2.052 |
| Aug | 8 | 0.515 | 2.052 |
| Sep | 9 | 0.417 | 2.312 |
| Oct | 10 | 0.363 | 2.460 |
| Nov | 11 | 0.333 | 2.484 |
| Dec | 12 | 0.311 | 2.554 |

where $\phi$ is the locations latitude, and $\delta$ is the declination angle, and $\omega$ is the hour angle.

The equation for calculating the declination angle for a non-leap year is given as (Myers, 2013):

$$\delta = 23.45 \sin\left[\left(\frac{360^o}{365}\right)(284 + n)\right] \quad (30)$$

The hour angle ($\omega$) is given by:

$$\omega = 15^o(T_{sh} - 12) \quad (31)$$

where $T_{sh}$ is the solar time (in hours).

For a known local standard time in hours, $T_{lh}$, the solar time in hours, $T_{sh}$, for that location is defined as (ASHRAE, 2017):

$$T_{sh} = T_{lh} + (\psi_a - \psi_s)/15 + E_{th} \quad (32)$$

where,

$\psi_s$ = the standard longitude angle (corresponding to the time zone), in degrees, for the location,

$\psi_a$ = the actual longitude angle, in degrees, for the location,

$T_{lh}$ = the local standard time, in hours.

The equation of time in seconds, $E_{ts}$ ($E_{ts} = 3600E_{th}$), is given as (Myers, 2013)

$$E_{ts} = (432/\pi)[0.0075 + 0.1868\cos\Gamma - 3.2077\sin\Gamma - 1.4615\cos 2\Gamma - 4.089\sin 2\Gamma] \quad (33)$$

where $\Gamma$ is defined as:

$$\Gamma = 360^o(n - 1)/365 \quad (34)$$

The local standard time is related to the standard longitude and the time zone ($T_z$) for a location as:

$$\psi_s = 15T_z \quad (35)$$

For the purpose of this simulation study, it is important to be able to compute the hour and at sunrise and sunset. The hour angles at sunrise ($\omega_{sr}$) and at sunset ($\omega_{ss}$) are the same numerically, however the sunrise hour angle is negative and the sunset hour angle is positive. The numerical value of the hour angle at sunrise (or sunset) hour angle can be calculated from:

$$\omega_s = cos^{-1}(-tan\phi tan\delta) \quad (36)$$

The total (global) solar irradiance reaching the solar still surface is $I$, and is the sum of the beam irradiance and the diffuse irradiance, i.e.:

$$I_G = I_b + I_d \quad (37)$$

***2.2.1 Solar Irradiance absorbed by solar still components***

The components of global incident irradiance absorbed by glass ($I_{ag}$), water mass ($I_{aw}$) and basin liner ($I_{ab}$) are defined in terms of glass absorptance ($\alpha_g$) and reflectance ($r_g$), and water absorptance ($\alpha_w$) and reflectance ($r_w$), as follows (Tiwari, 2002):

$$I_{gg} = c_g I(t) \quad (38)$$

$$I_{gw} = c_w I(t) \quad (39)$$

$$I_{gb} = c_b I(t) \quad (40)$$

Where the expressions for calculating $a_g$, $a_g$ and $a_g$ are given in Table 7 below.

Table 7: Expressions for calculating $\boldsymbol{a_g}$, $\boldsymbol{a_g}$ and $\boldsymbol{a_g}$ **(Tiwari, 2002)**

| Terms | Evaluating expressions |
|---|---|
| $c_g$ | $(1-r_g)\alpha_g$ |
| $c_w$ | $(1-\alpha_g)(1-r_g)(1-r_w)\alpha_w$ |
| $c_b$ | $(1-\alpha_g)(1-\alpha_w)(1-r_g)(1-r_w)\alpha_b$ |

**2.3. Models of ambient temperature**

The ambient temperature can be obtained from the empirical relation (ASHRAE, 2017):

$$T_a = T_{max} - f_h(T_{max} - T_{min}) \quad (41)$$

where $f_h$ is the hourly fraction of the daily temperature range. The fraction value varies during the day and the value for each hour of the day is given in Table 8 (ASHRAE, 2017):

**2.4. Instantaneous yield and efficiency of solar still**

The evaporation energy transfer from water to glass ($\dot{q}_{ewg}$) determines the yield of the solar still.

Table 8: Hourly fraction of the daily temperature range **(ASHRAE, 2017)**

| Time (h) | Fraction ($f_h$) | Time (h) | Fraction ($f_h$) | Time (h) | Fraction ($f_h$) |
|---|---|---|---|---|---|
| 1 | 0.88 | 9 | 0.55 | 17 | 0.14 |
| 2 | 0.92 | 10 | 0.38 | 18 | 0.24 |
| 3 | 0.95 | 11 | 0.23 | 19 | 0.39 |
| 4 | 0.98 | 12 | 0.13 | 20 | 0.50 |
| 5 | 1.00 | 13 | 0.05 | 21 | 0.59 |
| 6 | 0.98 | 14 | 0.00 | 22 | 0.68 |
| 7 | 0.91 | 15 | 0.00 | 23 | 0.75 |
| 8 | 0.74 | 16 | 0.06 | 24 | 0.82 |

Thus the instantaneous yield of the solar still in kilogram per second ($\dot{m}_{ew}$) is given as:

$$\dot{m}_{ew} = \frac{\dot{q}_{ewg} L_s B_s}{L} = \frac{h_{ewg} L_s B_s (T_w - T_g)}{L} \quad (42)$$

The instantaneous efficiency of the solar still ($\eta_i$) is given as:

$$\eta_i = \frac{\dot{q}_{ewg}}{I_{THG}} = \frac{h_{ewg}(T_w - T_g)}{I_{THG}} \quad (43)$$

# 3. RESULTS AND DISCUSSIONS

First, the models for the ambient temperature and global irradiance are simulated using the nominal values in Table 9.

Table 9: Parameters and their nominal values

| Symbol | Description | nominal value |
|---|---|---|
| $I_{SC}$ | Solar constant ($W/m^2$) | 1366 |
| $\psi_s$ | Standard longitude for the location | 15 |
| $\psi_a$ | Actual longitude of the location | 8.592 |
| $\phi$ | Latitude angle | $12.0^o$ |
| $n$ | nth day of the year ( | 105 |

The simulation codes and procedure is the subject of a follow-up article to this one. The latitude and longitude values in the table represent those of the chosen location, Kano, Nigeria, for the period between sunrise and sunset on 15th of April. The trends of the simulated ambient temperature and global irradiance are shown in Figure 2.

The figure shows that between sunrise and sunset on the chosen day, the global irradiance values are symmetrical about the solar noon (Figure 2b), while the ambient temperature values are not (Figure 2a). For example, at sunset when the global irradiance is zero, just as it was at sunrise, the ambient temperature at sunset is higher than the value at sunrise. These trends are in line with predictions and guidelines specified in (ASHRAE, 2017).

However, in the absence of verifiable daily solar irradiance data for Kano, one can only compare with monthly average irradiation data. The simulated irradiance for the chosen

date translates to daily irradiation value of 35.31 MJ/m$^2$. This is clearly higher than the reported daily average irradiation value for April, which is reported to be between 20-25 MJ/m$^2$ day (Muhammad & Darma, 2014)), (Mustapha & Mustafa, 2019) This is expected as the assumption is that of clear sky.

Next the solar still models are simulated using the simulated values of global irradiance and ambient temperature as inputs As already stated, the codes and simulation procedure are the subject to a follow-up paper to this. The models are simulated using the nominal parameter values of Table 10. The trends of the simulated solar still performance indices (water temperature, instantaneous depth of water, cumulative distillate yield and instantaneous efficiency) are as shown in Figure 3. The trends show that for a system operated between sunrise and sunset, the water temperature may theoretically reach 80$^o$C (Figure 3a), the distillate yield may be up to 8 kg/m$^2$ (Figure 3c) and that instantaneous efficiency may be more than 60% (Figure 3d), for a still of 1 m$^2$ water surface area. The instantaneous efficiency of the solar still increases with time from sunrise. The spike shown by the efficiency plot (Figure 3d) indicates that even towards sunset, when the irradiance is significantly low, distillate production continues because of the already elevated temperature of water, and its increased thermal capacitance, and the heat of evaporation. Hence at this region, distillate yield is very high relative to the global irradiance. These trends may depend on the specifics of the solar still in terms of variable inputs and materials of construction.

The trends largely follow the pattern of those presented in some previous works (Afrand, et al., 2017), (Hafs, et al., 2021), though these trends can be greatly affected by certain variables of the solar still such as the water mass (Khalifa & Hamood, 2009)

Table 10: Solar still fixed parameters and their nominal values

| Symbol | Description and unit | Nominal values |
|---|---|---|
| $L_s$ | length of still $(m)$ | 1 |
| $B_s$ | breadth of still $(m)$ | 1 |
| $d_{wg}$ | water-glass spacing $(m)$ | 0.25 |
| $t_i$ | insulator thickness $(m)$ | 0.005 |
| $t_g$ | glass thickness $(m)$ | 0.003 |
| $t_b$ | absorber thickness $(m)$ | 0.005 |
| $g$ | acceleration due to gravity $(m/s^2)$ | 9.81 |
| $k_i$ | Thermal conductivity of insulation $(W/m\,K)$ | 0.04 |
| $h_i$ | combined heat transfer coefficient from insulator $(W/m^2\,K)$ | 5.7 |
| $L$ | Latent heat of vaporisation of water $(J/Kg)$ | 2256700 |
| $v_a$ | velocity of air $(m/s)$ | 3 |
| $C_{pg}$ | specific heat capacity of glass $(J/kg\,K)$ | 750 |
| $C_{pb}$ | specific heat capacity of basin liner (absorber) $(J/kg\,K)$ | 385 |
| $\rho_g$ | density of glass $(kg/m^3)$ | 2800 |
| $\rho_b$ | density of basin liner $(kg/m^3)$ | 8933 |
| $\theta$ | Slope of glass cover (degrees) | 11 |
| $\sigma$ | Stephan-Boltzmann constant | 5.67e-8 |
| $C_f$ | Basin-water convective heat transfer constant (lamina flow | 0.54 |
| $n_f$ | Basin-water convective heat transfer index (lamina flow | 0.25 |
| $\varepsilon_g$ | Emissivity of glass | 0.9 |
| $\varepsilon_w$ | Emissivity of water | 0.9 |
| $r_g$ | Reflectivity of glass | 0.08 |
| $r_w$ | Reflectivity of water | 0.1 |
| $\alpha_g$ | Absorption coefficient of glass | 0.02 |
| $\alpha_w$ | Absorption coefficient of water | 0.03 |
| $\alpha_b$ | Absorption coefficient of basin | 0.9 |

ISSN: 2449 - 0539
BAYERO JOURNAL OF ENGINEERING AND TECHNOLOGY VOL 18 NO. 2 MAY 202 PP. 104-112

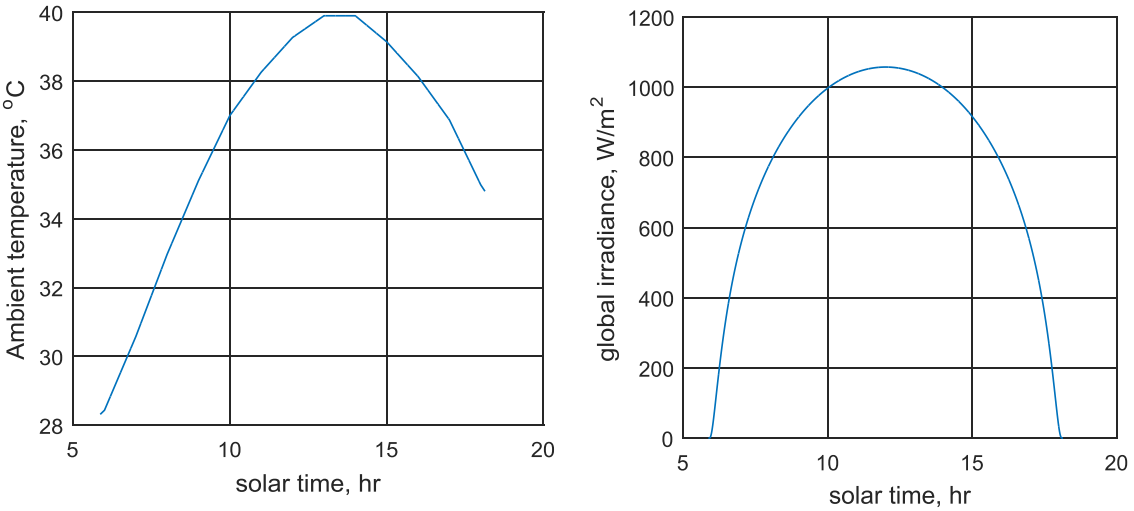


(a) (b)

Figure 2: Plots of simulated ambient temperature (a) and global irradiance (b)

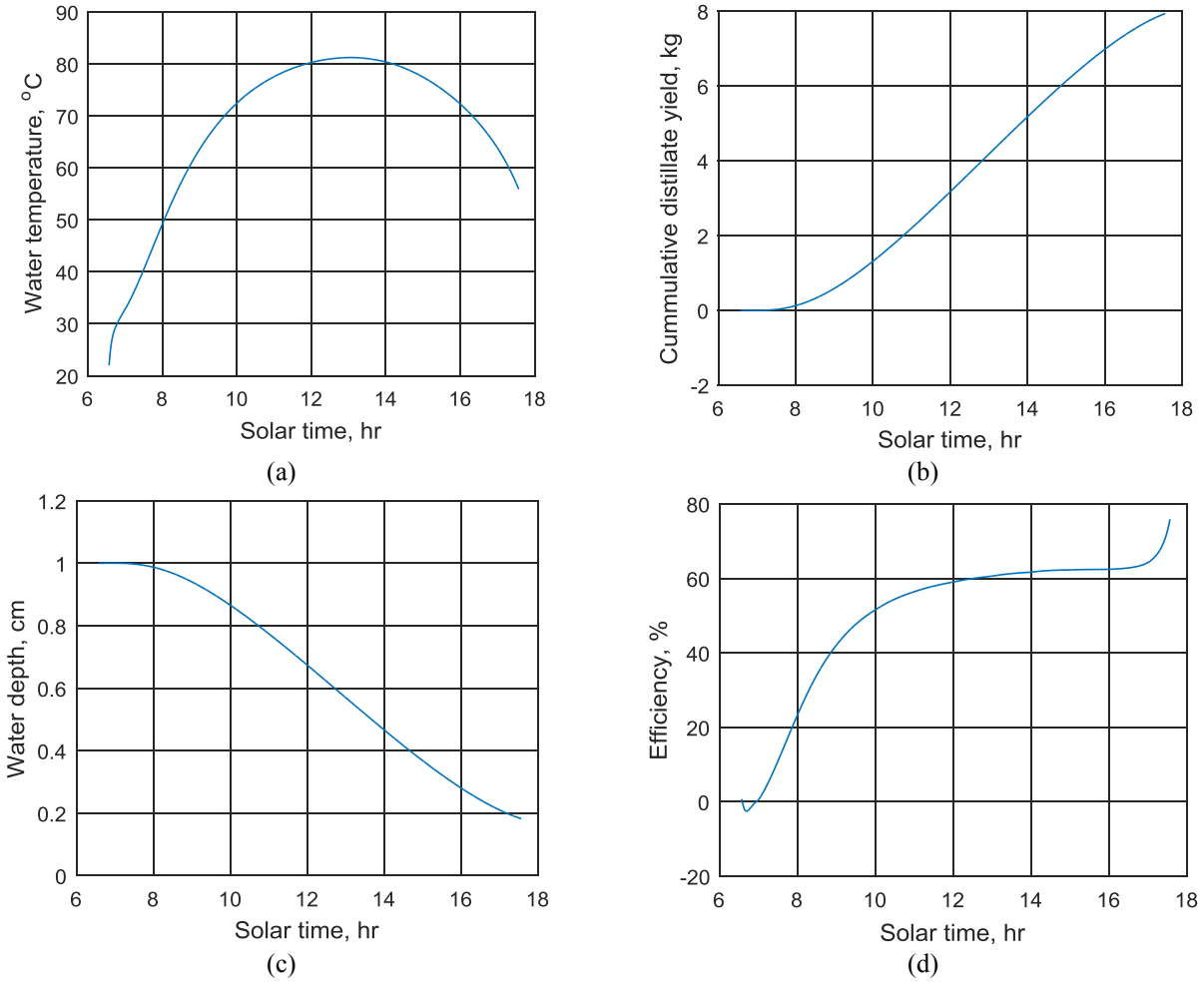


(a) (b) (c) (d)

Figure 3: Trends of simulated solar still performance indices

.

# 4. CONCLUSIONS

The mathematical models for single-slope solar still has been presented, together with the models for estimating the ambient temperature and global irradiance. The solar still models are presented as transient phenomena with regards to many variables: the ambient temperature, the global irradiance, seasonal variations, the water mass and even some properties of the still such as thermal capacitance of water. This transient approach gives a clearer picture of per second characteristics of the variables within a period, as opposed to steady state approach which only gives a total sum after the period. In this case the effects of these variables on the performance of the still can be studied as they vary with time. Also, the effects of other parameters such insulation type and thickness, glass cover type, absorber type, and many others, can be studied with these models.

# REFERENCES

Afrand, M., Kalbasi, R., Karimipour, A. & Wongwises, S., 2017. Experimental investigation on a thermal model for basin solar still with an external reflector. *Energies,* 10(18), pp. 1-16.

ASHRAE, 2017. *ASHRAE Handbook Fundamentals (SI Edition).* s.l.:s.n.

Cooper, P. I., 1969. Digital simulation of transient solar still processes.. *Solar Energy,* Volume 12, pp. 313-333.

Duffie, J. A. & Becham, W. A., 2013. *Solar Engineering of Thermal Processes.* 2013: Willey.

Dunkle, R. V., 1961. *Solar Distillation: the roof type still and a multiple effect diffusion still.* Colorado, International Development in Heat Transfer, p. 895.

Dwivedi, V. K. & Tiwari, G. N., 2009. Comparison of internal heat transfer coefficients in passive solar still by different thermsl models: an experimental validation.. *Desalination,* pp. 304-318.

Ebaid & Ammari, 2015. Modelling and analysis of unsteady-state thermal performance of a single-slope tilted solar still. *Renewables: wind, water and solar,* pp. 2-19.

El-Sebaila, A. & Al-Dossarib, M., 2011. A mathematical model of single basin solar still with an external reflector. *Desalination and Water treatment,* Volume 26, pp. 250-259.

Fernandez, J. L. & Chargoy, N., 1990. Multistage indirect heated solar still. *Solar energy,* 44(4), pp. 215-223.

Frick, B., 1970. *Some New Considerations about Solar Stills.* Melbourne, s.n., p. 395.

Gupta, B., Mandraha, T. K., Edla, P. J. & Pandya, M., 2013. Thermal modelling and efficiency of solar water distillation: a review. *American Journal of Engineering Research,* 02(12), pp. 203-213.

Hafs, H. et al., 2021. Numerical simulation of the performance of passive and active solar still with corrugated absorber surface as heat storage medium for sustainable solar desalination technology. *Groundwater for Sustainable Development,* Volume 14, pp. 1-17.

Johnson, A. et al., 2019. A thermal model for predicting the performance of a solar still with Fresnel Lense. *Water,* pp. 1-20.

Kasten, F. & Young, A. T., 1989. Revised optical air mass tables and approximation formula. *Applied Optics,* 28(22), pp. 4735-4738.

Khalifa, A. & Hamood, A., 2009. On the verification of the effect of water depth on the performance of basin type solar stills.. *Sol. Energy,* 83(8), p. 1312–1321.

Lof, G. O. G., Eibling, J. A. & Bloemer, J. W., 1961. Energy Balances in Solar Distillers. *America Institute of Chemical Engineers Journal,* 7(4), p. 461.

McMullan, J. T., Morgan, R. & Murray, R. B., 1990. *Energy Resources.* 2nd ed. London: Edward Arnold.

Muhammad, A. & Darma, T. H., 2014. Estimation of Global Solar Radiation for Kano State Nigeria Based on Meteorological Data. *.IOSR Journal of Applied Physics ·(IOSR-JAP),* 6(6), pp. 19-23.

Mustapha, M. & Mustafa, M. W., 2019. Estimation of global solar irradiation on horizontal surface in Kano, Nigeria, using air temperature amplitude. *International Journal of Integrated Engineering,* 11(6), pp. 103-109.

Myers, D. R., 2013. *Solar Radiation Practical Modelling for Renewable Energy Applications.* New York: CRC Press, Taylor & Francis Group.

Nayak, J. K., Tiwari, G. N. & Sohha, M. S., 1980. Periodic Theory of Solar Still. *International Journal of Energy Research,* Volume 4, p. 41.

Tiwari, G. N., 2002. *Solar Energy: Fundamentals, Design, Modelling and Applications.*. New Delhi: Narosa Publishing House.

Torchia-Núñez, J. C., Cervantes-de-Gortari, J. & Porta-Gándara, M. A., 2014. Thermodynamics of a Shallow Solar Still,. *Energy and Power Engineering,* Volume 6, pp. 246-265.

Watmuff, J. H., Chaters, W. W. S. & Proctor, D., 1977. Solar and wind induced external coefficients for solar collectors. *Revue Intetnationale d'Eleliotechnique,* 6(56).

Yeo, K. B., Ong, C. M. & Teo, T. K., 2014. Heat transfer energy balance model of single slope solar still. *Journal of Applied Sciences,* 14(23), pp. 3344-3348.